# Final Technical Report

During the past decades, considerable theoretical efforts have been devoted to studying the electronic and geometric structures and related properties of surfaces. Such efforts are particularly important for systems like the actinides for which experimental work is relatively difficult to perform due to material problems and toxicity. The actinides are characterized by a gradual filling of the 5f-electron shell with the degree of localization increasing with the atomic number Z along the last series of the periodic table. The open shell of the *5f* electrons determines the atomic, molecular, and solid state properties of the actinide elements and their compounds and understanding the quantum mechanics of the *5f* electrons is the defining issue in the chemistry and physics of actinide elements. These elements are also characterized by the increasing prominence of relativistic effects and their studies can, in fact, help us understand the role of relativity throughout the periodic table. However, the electronic and geometric structures of the actinides, specifically the trans-uranium actinides and the roles of the 5f electrons in chemical bonding are still *not* well understood. This is crucial not only for our understanding of the actinides but also for the fact that the actinides constitute “the missing link” between the d transition elements and the lanthanides. The *5f* orbitals have properties intermediate between those of localized 4f and delocalized 3d orbitals. Thus, a proper understanding of the actinides will help us understand the behavior of the lanthanides and transition metals as well. In fact, there is an urgent need for continued e*xtensive and detailed* theoretical research in this area to provide significant and deep understandings of the electronic and geometric structures of the actinides.

In this work, we have performed electronic structure studies for plutonium (Pu), americium (Am), and curium (Cm) surfaces, and molecular adsorptions on Pu and Am surfaces. In particular, the region at the boundary of Pu and Am, is widely believed to be the crossover region between d-like itinerant and f –like localized behavior The eventual goal is a complete understanding of the surface chemistry and physics processes of *all* actinide surfaces, defining the chemistry and physics of such heavy elements. Among the actinides, plutonium, with five *5f* electrons in the solid state, is arguably the most complex, fascinating, and enigmatic element known to mankind and has attracted extraordinary scientific and technological interests because of its unique properties, generating a significant body of research in diverse areas, including superconductivity. Pu has, at least, six stable allotropes between room temperature and melting at atmospheric pressure, indicating that the valence electrons can hybridize into a number of complex bonding arrangements. Central and critical questions relate to the electronic structure, localization of the 5*f* electrons and the magnetism of Pu. For the light-actinides, from Th to Pu, the *5f* electrons are believed to be delocalized, hybridizing with the 6d and 7s electrons. For the heavier actinides, Am and beyond, the *5f* electrons are localized with the *5f* orbitals progressively lower in energy relative to the 6d configuration. Hence, Pu is in a position where the *5f* electronic behavior changes from itinerant to localized. As far as magnetism is concerned, a majority of the theoretical calculations continues to claim the existence of magnetism while almost all the experimental results do not find any support for such claims. The *second* element of interest to us, namely americium, occupies a central position in the actinide series with respect to the involvement of *5f* electrons in metallic bonding. It is widely believed that the 5*f* electrons in Am are localized and that Am undergoes a series of crystallographic phase changes with pressure. Fully-relativistic all electron surface studies of the different phases of Am, *initially* for the dhcp and the fcc surfaces, can and have provided us with valuable information about chemical bonding in Am and the transitions from f-electron delocalization to f-electron localization in trans-uranium compounds. In particular, a comparative study of the electronic structures of the Pu and Am surfaces using the techniques of all-electron modern

density functional theory *and beyond* can provide significant information about the role of *5f* electrons in bond formation as also the localization of the *5f* electrons, matters of considerable controversies. The change from metallic *5f* bonding into local-moment nonbonding configurations that takes place between Pu and Am is rather unique in the periodic table and is at the very heart of our understanding of electronic structure. We believe that, considering the narrow bandwidth of surface states, any transition from itinerant to localized behavior first takes place at the actinide surfaces with possible reconstructions and one purpose of our current work is to study these surfaces by representing them with a series of layers to understand these transitions.

We hasten to point out that almost three decades after the conference on trans-plutonium elements, actinide surface chemistry and physics remain, to date, *a largely unexplored field being pursued by a very limited number of research groups across the world* and an opportunity exists here to understand and pinpoint how and why this transition from itinerant transition-metal-type to localized lanthanide-type system takes place and what factors determine the changeover. This, in reality, is actually a question not only of actinide electronic structures but also a question about electronic structure theory in general. A parallel opportunity also exists here for us to understand how electron correlations affect bonding and lattice structures and how we can progress beyond one-electron band theories. This has important implications for the physics and chemistry of all elements in the periodic table in that it might pave the way for a unified electron theory of solids. The *third* element of interest in our research is curium. This element is at the center of the actinide series and has a half-filled shell with seven 5*f* electrons. At ambient pressure, the structure is double hexagonal close packed and with application of pressure, the dhcp structure changes to fcc. This element has not been studied in detail as far as the published literature is concerned. We believe a comparative study of Am and Cm would provide us with further insights about the properties of the presumably localized 5*f* electrons.

The second approach to study chemical bonding in these surfaces is through atomic and molecular adsorption studies on a series of carefully selected actinide substrates. Also, it is worth pointing out that studies of the reactions of the actinides with atomic and molecular systems are critically important for environmental reasons, since, for example, according to the U. S. Government, about fifty tons of Pu is surplus to U. S. needs and should be set aside for eventual disposition. Thus our studies of Pu, Am, and Cm surfaces and atomic and molecular adsorptions on such, as detailed below, not only help us understand and explain fundamental heavy element chemistry and physics with implications across the entire range of the periodic table but that such a study might also guide us towards a safe disposition of actinide elements like plutonium when necessary. All work mentioned in this proposal has been carried out at the University of Texas at Arlington and the Texas Advanced Computing Center (TACC) in Austin.

The current project was funded from September 1, 2006 to August 31, 2010. During this period, we have completed the following studies, using the computational formalisms of modern density functional theory and variants thereof as implemented in the suite of software *WIEN2k* and *DMOL*$^3$ : ***a**) Relativistic Studies of Atomic Carbon and Oxygen Adsorptions on the (100) Surface of γ – U; **b**) Relativistic Studies of CO Molecule Adsorptions on the (100) Surface of γ – U; **c**) Relativistic Studies of Atomic Carbon, Nitrogen, and Oxygen Adsorptions on the δ-Pu (111) and δ – Pu (100) Surfaces; **d**) Relativistic Studies of the Relaxation of the (111) Surface of δ – Pu and Effects on Atomic Adsorption; **e**) Molecular and Dissociative Adsorptions of Water Molecule on the δ-Pu (111) Surface; **f**) Molecular and Dissociative Adsorptions of Carbon Dioxide Molecule on the δ-Pu (111) Surface; **g**) Relativistic Studies of Atomic Carbon, Nitrogen, and Oxygen Adsorptions on the α – Pu (020) Surface; **h**) Hybrid Density Functional Study of*

*FCC δ – Pu; **i**) Hybrid Density Functional Study of DHCP Am; **j**) LDA+U Study of DHCP Am and Cm; **k**) Relativistic Density Functional Study of the Actinide Nitrides; **l**) Relativistic Studies of DHCP and FCC Surfaces of Am; **m**) Atomic Hydrogen and Oxygen Adsorptions on the (0001) Surface of DHCP Am; **n**) Molecular and Dissociative Hydrogen and Oxygen Adsorptions on the (0001) Surface of DHCP Am; **o**) Molecular and Dissociative Adsorptions of Water Molecule Adsorption on the (0001) Surface of DHCP Am; p) Molecular Adsorption Studies on α – Pu (020) Surface; q) Studies of Actinide Oxide Compounds.* All work has been performed with graduate students and postdoctoral fellows at the University of Texas at Arlington (UTA).

For the sake of brevity, we will comment only on *some* of our representative works and only on the *basic* conclusions from these works. Though the grant has officially expired, we continue to work on this project of fundamental scientific, technological, environmental, and societal importance.

**a) <u>Atomic Adsorptions on the δ - Pu (111) and (100) Surfaces</u>**

For atomic C, N, and O adsorptions on the δ-Pu (111) surface (adsorption sites shown in Fig. 1), the hollow fcc adsorption site was found to be the most stable site in all cases with chemisorption energies for C, N, and O being 6.539 eV, 6.714 eV, and 8.2 eV respectively. The respective distances of the C, N, and O adatoms from the surface were found to be 1.16 Å, 1.08 Å, and 1.25 Å. Our calculations indicate that SOC has negligible effect on the chemisorption geometries but energies with SOC are more stable than the cases with NSOC within a range of 0.05 to 0.27 eV. The work function and net magnetic moments respectively increased and decreased in all cases upon chemisorption compared with the bare δ-Pu (111) surface. In Figure 2, plots for the 5*f* and 6*d* density of states (DOS) are shown for the clean slab (Figure 2a), C adsorbed on the surface, which is the least reactive (Figure 2b), and O adsorbed on the surface, which is the most reactive (Figure 2c). Clearly, in comparison to the clean slab, the 5*f* bands near the Fermi level for least stable top site broaden significantly after adsorption implying 5*f* delocalization. For the most stable hollow sites, the shape and character of the 5*f* bands remains virtually unchanged. We thus infer that the participation of the 5f states in bonding destabilizes the Pu-adsorbate interaction.

We also studied the effects of relaxation of this surface. The relaxation energy, which is defined as the total energy before relaxation minus the total energy after relaxation, was 1.04 mRy, indicating the fair stability of the surface. In Figure 3, we show plots of the difference charge density to study the nature of the bond. For the top site, we clearly see excess charge build-up around the O adatom. Also, a polarization towards the nearest neighbor Pu atom can be seen. Overall, the bond has a strong ionic character. For the bridge and hollow sites, significant charge accumulation around the O adatom can clearly be seen with charge depletion around both Pu atoms along the Pu-O bonds. This again suggests that bonding is primarily ionic.

For atomic C, N, and O adsorptions on the δ-Pu (100) surface, for all chemisorption processes, the hollow site (also known in this case as the center site) adsorption site was found to be the most preferred site with SOC chemisorption energies of 7.964 eV, 7.665 eV, and 8.335 eV for the C, N, and O adatoms, respectively. The respective distances of the C, N, and O adatoms from the surface were found to be 0.26 Å, 0.35 Å, and 0.48 Å. As was the the case for (111) surface, the work functions and the net magnet moments respectively increased and decreased in all cases compared with the bare δ-Pu (100) surface. In particular, the work function shift is largest for the least preferred top site and lowest for the most preferred center

site. The nature of the bonding between the surface Pu atoms and the adatoms was found to be largely ionic.

**b) Adsorptions of water on the δ-Pu (111) surface**

The adsorption of water molecule on the δ – Pu (111) surface have been studied in molecular $H_2O$, partially dissociated OH+H, and completely dissociated O+H+H configurations. The calculations were done in a two-step process: first, ionic positions were relaxed using the *DMol*[3] code and then the DMol[3]-optimized structures were used as inputs for full self-consistent *WIEN2k* runs. A 5-layer δ-Pu (111) surface was used. The orientation of the water molecule with respect to the surface, α, is shown in Figure 4. α is the angle between the water dipole moment and the surface.

The water molecule was initially placed in three orientations, namely, α=-90°, 90°, and 0°. It was observed that the adsorption process is clearly physisorptive, with the most stable configuration corresponding to an adsorption energy of 0.59 eV. Secondly, the water molecule in all cases relaxes from an initial non-*top* site to the neighboring *top* site or stays at the initial *top* site. Also, the molecule relaxes from their initial state (orientation) $\alpha_i$ = -90°, 0°, 90° to a final state $\alpha_f$ =9° to12°, which implies that $H_2O$ molecule prefers to adsorb on-top with nearly flat lying dipole moment relative to the surface. The adsorbate-to-substrate charge transfer can clearly be seen in difference charge density plot in Figure 5a and Figure 5b indicates the local density of states illustrating the Pu *6d* interaction with the water highest occupied molecular $1b_1$ orbital. In Figure 5c, we show the energy profile of $H_2O$ diffusion across the surface along the top-bridge-top route. This route is the lowest energy pathway for diffusion across the surface. IS is the initial state, TS is the transition state, and FS is the final state. The barrier to diffusion, $E_b$, is predicted to be 0.18 eV.

For co-adsorption of H and OH, we found that the most energetically plausible configuration corresponds to both H and OH at neighboring $F_3$ sites or neighboring $H_3$ sites. We found that the binding energies are nearly degenerate with the molecule preferring a $\alpha_f$ =90° orientation. The chemisorption energies of 5.16 eV to 5.19 eV are about an order of magnitude larger than the molecular physisorption energies. The OH bond lengths contract by 0.02 Å-0.03 Å and the top layer usually expands significantly compared to the bare surface. The re-arrangement of the surface Pu atoms to accommodate the adsorbates leads to surface rumplings of Δr = 0.20 Å to 0.93 Å. Coordination number plays an important role in the stabilization of chemisorbed system, with higher coordination number usually implying stronger binding.

Simulation of the fully dissociated products was carried out by placing each product at neighboring $F_3$ sites or at neighboring $H_3$ sites. The adsorption energies for the fully dissociated product is more stable than that of the partially dissociated products, which in turn is more stable than that of the molecule. The average relaxation of the top layer is surprisingly small. However, rumplings of the surface layer are quite significant. This is because at such a high coverage of 75%, the substrate must undergo significant structural rearrangements to accommodate the three adsorbates. The range of the bond distances and the three-fold coordination of each atom guarantee maximum adsorbate-substrate overlap and hence the binding is expected to be more stable.

In Figures 5d and 5f, the difference charge density plots for (OH+H)/δ-Pu(111) system and (O+2H)/δ-Pu(111) systems are shown. Clearly the O-Pu and H-Pu bonds in both figures are mainly ionic in character since there is a significant displacement of charge density from Pu

towards the O and atomic H and the OH molecule is polarized. The dipoles formed on the O-Pu and H-Pu bonds will point towards the surface at an angle while the dipole formed on the upright O-H bond will point out of the surface. In case, a straightforward quantification of the alignment of induced net dipole moment is not possible and we rely on the work function to predict its orientation. The LDOS are shown in Figures 5e and 5g.

.

**c) Adsorption of carbon dioxide on the δ-Pu (111) surface:**

Three initial orientations of the $CO_2$ molecule were considered: (i) along the surface normal; (ii) parallel to the lattice vector (hor1); (iii) perpendicular to the lattice vector (hor2). For an initially vertically oriented $CO_2$ molecule, the binding is extremely weak at the NSOC level (0.06-0.14 eV) or no binding at SOC level (-0.06-0.01 eV). With the molecule initially lying flat on the surface, chemisorption takes place with the $CO_2$ molecule spontaneously dissociating from the atop site into CO+O in one case, while in all other cases, the molecule had a bent structure with O-C-O bond angles between 118º and 130º. As an example, an initially flat lying molecule at the top site in the hor1 orientation transformed to a bent structure (Figure 6a), while the picture on the right in Figure 6b shows initially flat lying molecule at the top site in the hor2 orientation that spontaneously dissociates into $CO_2 \rightarrow CO+O$. The bond-bending of the molecule is due to the population of the $CO_2$ lowest unoccupied $2\pi_u$ orbital by the Pu 5*f*, 6*d* states. For CO+O co-adsorption, the most stable cases involve a tilt of the CO molecule with respect to the surface normal by 48º and an elongation of CO bond due to the population of the CO states and a hybridization of the CO 5σ and 1π states with the O 2p states. The picture on the left in Figure 7a shows DOS for the bare surface, that of the $CO_2$ and CO in vacuum, while Figure 7b on the right shows the bent $CO_2$ structure (hor1) and the dissociated products (hor2) on the surface. The modifications of the $CO_2$-$2\pi_u$ orbital as well as that of CO 5σ and 1π states can clearly be seen. For completely dissociative adsorption, significant O 2*p* and Pu 5*f*, and Pu 6*d* hybridizations lead to strong binding energies. Stability is characterized by anomalously large rumpling of the surface layer. Overall, the presence of the adsorbates induces delocalization in the Pu 5*f* electron states compared to the bare surface.

**d) Carbon, Nitrogen, and Oxygen Adsorptions on the α-Pu (020) surface**

The ground state of Pu, α-Pu, has been determined experimentally as a low symmetry monoclinic structure having a space group $P2_1/m$ with 16 atoms in the crystal unit cell. α-Pu, which is the most dense phase of Pu, is hard and brittle but soft vibrationally. For adsorption studies on the atomically flat (020) surface, a 4-layer slab with 8 Pu atoms per layer was used to model the surface. Adsorbates were placed on both faces of the slab to preserve inversion symmetry. Four distinct adsorption sites were identified on the α-Pu (020) surface. These are the one-fold top, one-fold hollow, two-fold short bridge, and two-fold long bridge sites (see Figure 8).

The short bridge site was the most stable adsorption site for C with chemisorption energies of 5.880 eV and 6.038 at the NSOC and SOC levels of theory, respectively. The long bridge site was the most stable adsorption site for N and O with chemisorption energies at the NSOC and SOC levels of theory being 5.806 eV and 6.067 eV for N and 7.155 eV and 7.362 eV for O, respectively. The respective distances of the C, N, and O adatoms from the surface for the most stable adsorption sites were found to be 1.32 Å, 1.26 Å, and 1.35 Å. Our results show that SOC adsorption energies are more stable than NSOC adsorption energies in the 0.14-0.32 eV range. The work function and net spin magnetic moments respectively increased and decreased in all cases upon chemisorption compared to the bare surface. A study of the local density of states indicates that at the least favorable top site a reduction occurs in the 5*f* DOS at

the Fermi level of the Pu atom on-top of which the adatoms sit implying further delocalization of the 5*f* electrons upon chemisorption. Significant Pu (6*d*)-Pu (5*f*)-adatom (2*p*) hybridizations are also observed in all cases.

**e) Hybrid Density Functional Theory Studies of δ-Pu and α-Am**

Using a hybrid functional, an NM ground state was realized for $\alpha$ =0.55 (α indicating the fraction of the HF exchange) but the equilibrium atomic volume deviated from experiment by 19%, the 5*f* electron population close to 4 (experimental value is close 5) and the 5*f* DOS that shows anomalous localization (see Figure 9a in the left panel) and obviously fails to match experimentally obtained PES data. Figs. 9b through 9e show the DOS for different values of α. The key conclusion of the work was that hybrid functional (at least for the PBE DFT functional) performs relatively worse on δ-Plutonium compared to pure DFT. On the other hand, by applying the hybrid functional to Americium I and systematically varying $\alpha$, we observed that for $\alpha \geq 0.29$, the ground state is NM, the error in the atomic volume is 4-11% and a constant 5*f* electron population is 5.8. More importantly, for $\alpha$ =0.40, the correct peak position in the 5*f* electron DOS (at around 3 eV below the Fermi level) matches qualitatively with experimental PES data (See Figs. 10a-10e). Thus our work shows the structural and electronic properties of Am can be determined using *ab initio* hybrid density functional theory. The results can then be compared with results using LDA+U or LDA+DMFT, both of which rely on the Hubbard parameter U (U is usually treated as adjustable and both methods are therefore strictly not *ab initio* schemes).

**f) Oxygen Adsorption on α – Pu (020) Surface**

Molecular and dissociative oxygen adsorptions on the α-Pu (020) surface have been systematically studied using the full-potential linearized augmented-plane-wave plus local orbitals (FP-LAPW+lo) basis method and the Perdew-Burke-Ernzerhof (PBE) exchange-correlation functional. Chemisorption energies have been optimized for the distance of the admolecule from the Pu surface and the bond length of O-O atoms for four adsorption sites and three approaches of $O_2$ admolecule to the (020) surface. Chemisorption energies have been calculated at the scalar-relativistic level with no spin-orbit coupling (NSOC) and at the fully relativistic level with spin-orbit coupling (SOC). Dissociative adsorptions are found at the two horizontal approaches ($O_2$ is parallel to the surface and perpendicular/parallel to a lattice vector). Hor2 ($O_2$ is parallel to the surface and perpendicular to a lattice vector) approach at the one-fold top site is the most stable adsorption site, with chemisorption energies of 8.048 and 8.415eV for the NSOC and SOC cases, respectively, and an O-O separation of 3.70 Å. Molecular adsorption occurs at the Vert ($O_2$ is vertical to the surface) approach of each adsorption site. The calculated work functions and net spin magnetic moments, respectively, increase and decrease in all cases upon chemisorption compared to the clean surface. The partial charges inside the muffin tins, the difference charge density distributions, and the local density of states have been used to investigate the Pu-admolecule electronic structures and bonding mechanisms.

**g) Water Adsorption on α – Pu (020) Surface**

Adsorptions of water in molecular ($H_2O$) and dissociative (OH+H, H+O+H) configurations on the α-Pu (020) surface have been studied using *ab initio* methods. The full-potential FP/LAPW+lo method has been used to calculate the adsorption energies at the scalar relativistic with no spin-orbit coupling (NSOC) and fully relativistic with spin-orbit coupling (SOC)

theoretical levels. It is found that the SOC effect increases the adsorption energies by ~0.30 eV for the two dissociative adsorptions. Weak physisorptions have been observed for the molecule $H_2O$ on the α-Pu (020) surface with primarily a covalent bonding, while the two dissociative adsorptions are chemisorptive with ionic bonding. The one-fold top site with an almost flat-lying orientation is found to be the most stable site for the adsorbed $H_2O$ molecule. At the SOC level, the most stable adsorption energy is 0.58eV, the corresponding values being 5.44 eV and 5.73 eV for the partial dissociation and complete dissociation cases, respectively. The analysis of the local projected density of states shows that the surface Pu-5f electrons remain primarily chemically inert in the molecular water adsorption process. Completely dissociative adsorption at a long bridge site for the dissociated O atom and two short bridge sites for the two dissociated H atoms is the most stable adsorption site. Hybridizations of O(2p)-H(1s)-Pu(5f)-Pu(6d) are observed for the two dissociative adsorptions, implying that some of the Pu-5f electrons become further delocalized and participate in chemical bonding. Work functions decrease for the molecular and the partial adsorption processes while it increases for complete dissociation.

**h) $CO_2$ Adsorption on α – Pu (020) Surface**

Adsorption of $CO_2$ on α-Pu (020) surface is investigated using GGA-DFT and the suite of software *DMOL*[3] and *WIEN2k.* Completely dissociated configurations (C+O+O) exhibit the strongest binding with the surface (7.94eV), followed by partially dissociated (CO+O) and molecular $CO_2$ configurations (5.18 and 1.90eV, respectively). For initial vertically upright orientations, final configuration of the $CO_2$ molecule does not change after optimization. For initial flat lying orientations, the final states correspond to bent geometry with a bond angle of ~130°. For CO+O co-adsorption, the stable configurations correspond to CO dipole moment orientations of 105°-167° with respect to the normal surface.

Figure 1

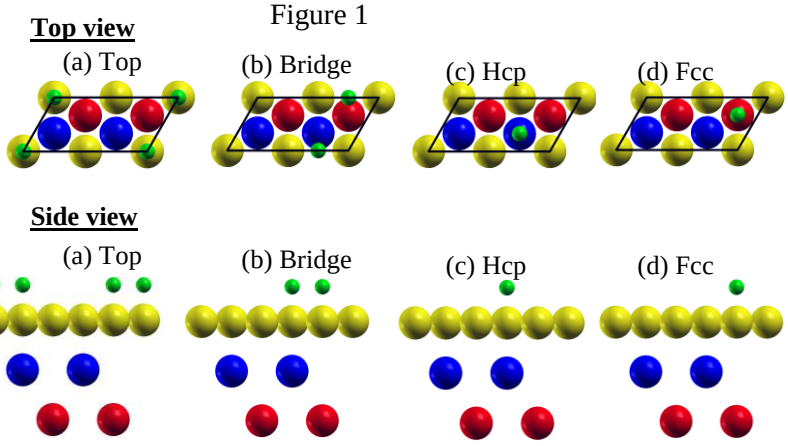


Figure 2a

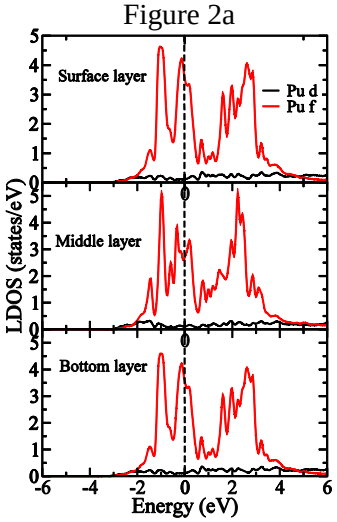


Figure 2b

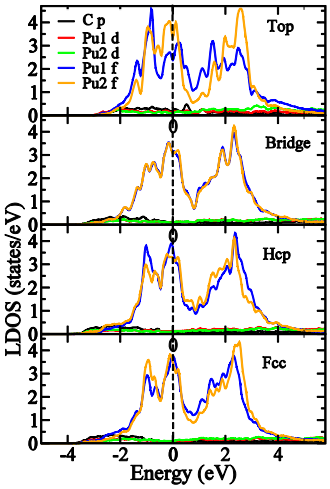


Figure 2c

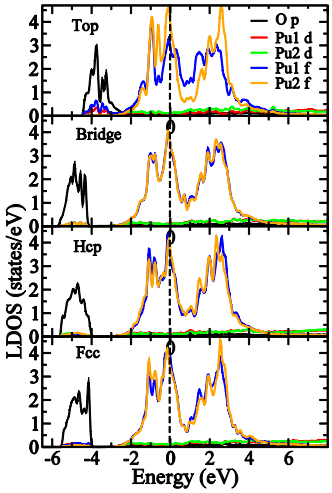


Figure 3

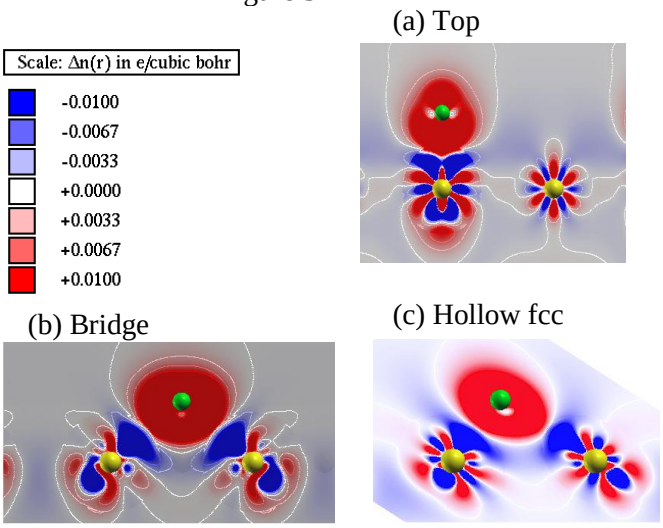


Figure 4

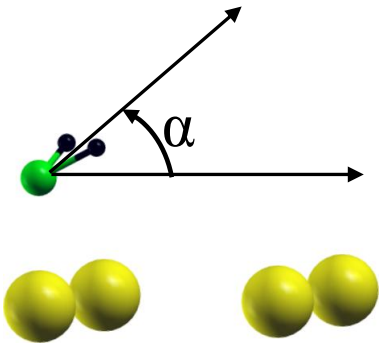

Figure 5a

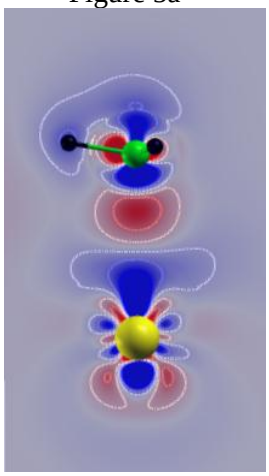

Figure 5b

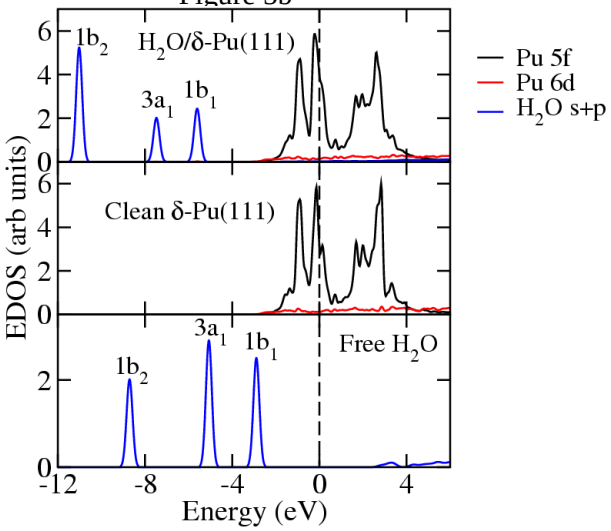


Figure 5c

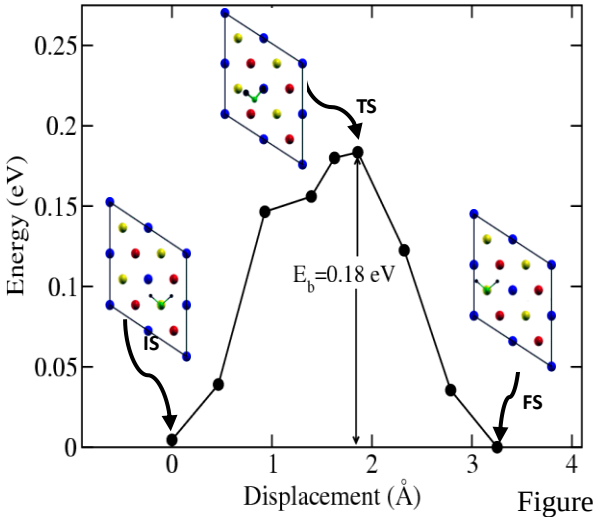


Figure 5d

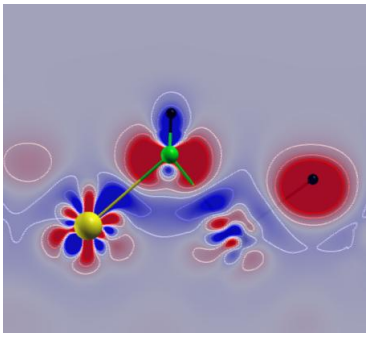

Figure 5e

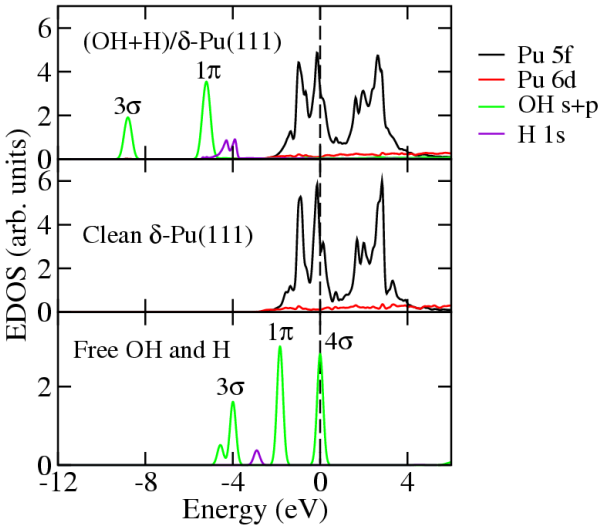

Figure 5f

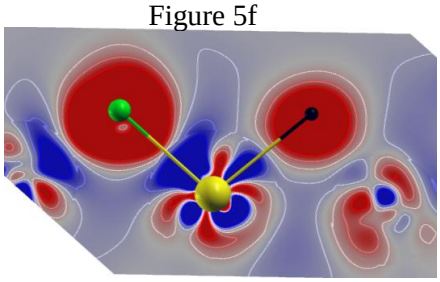

Figure 5g

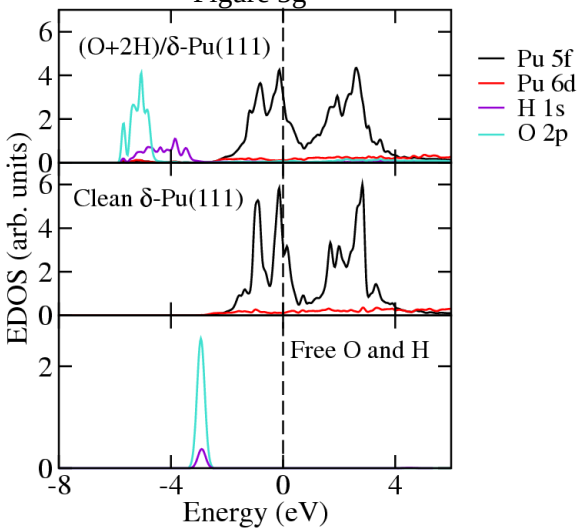


Figure 6a

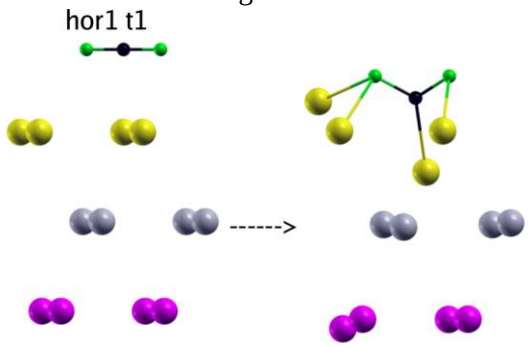


Figure 6b

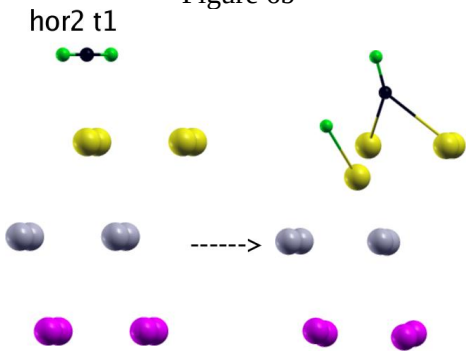


Figure 7a

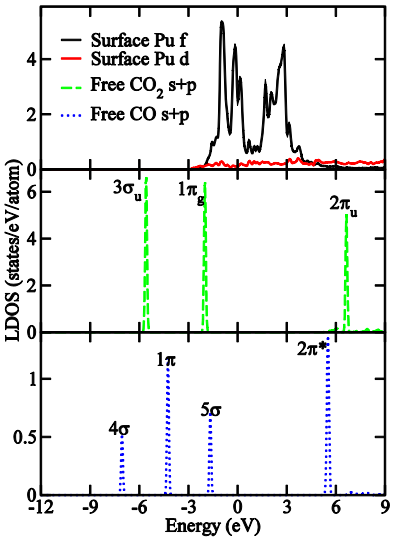


Figure 7b

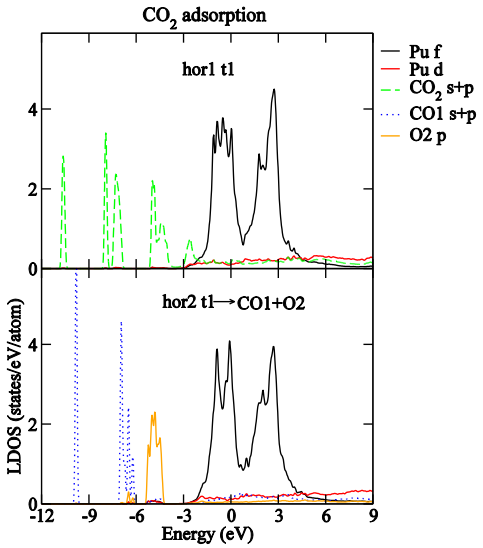

Figure 8

Top view

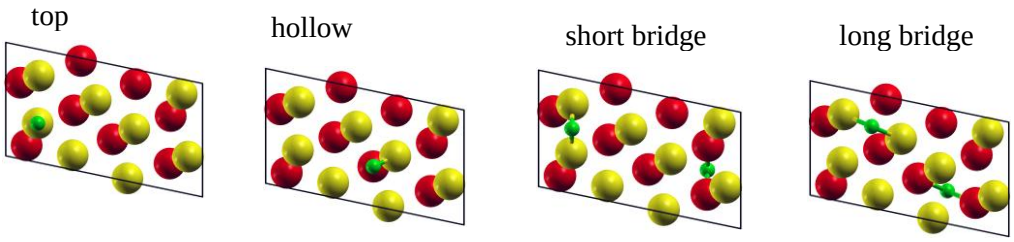


Side view

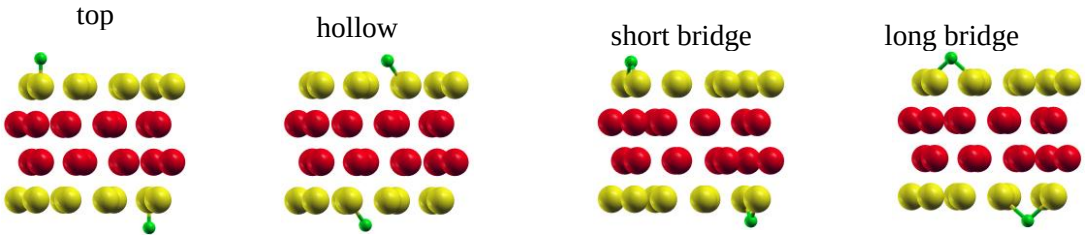


Figure 9a

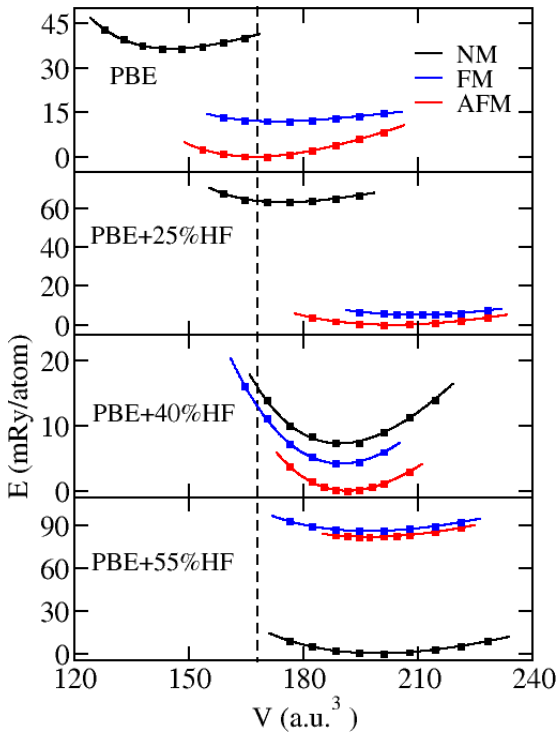


Figure 9b

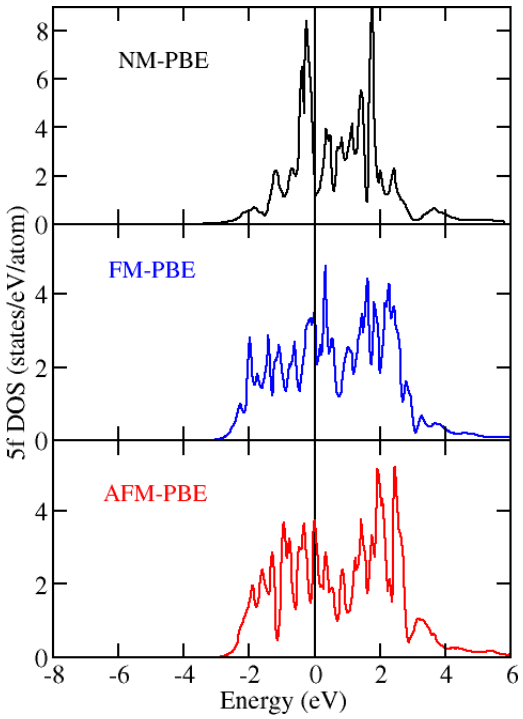

Figure 9c

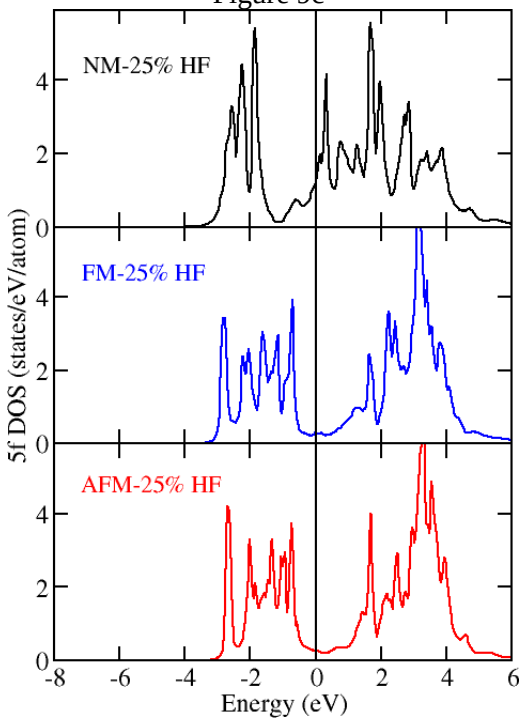


Figure 9d

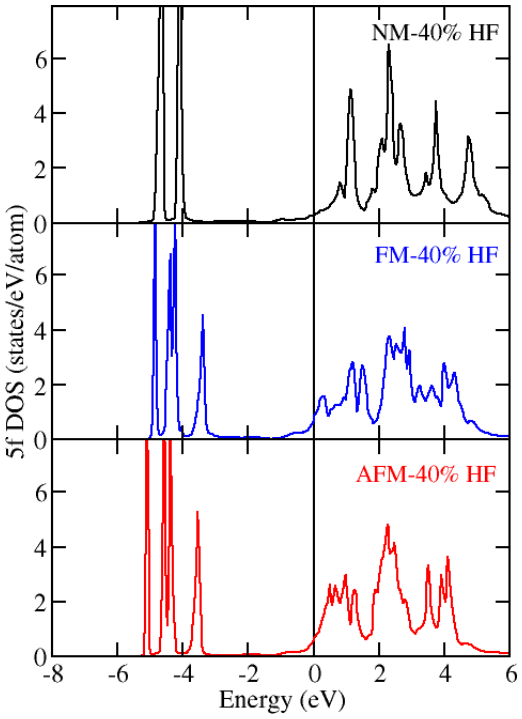


Figure 9e

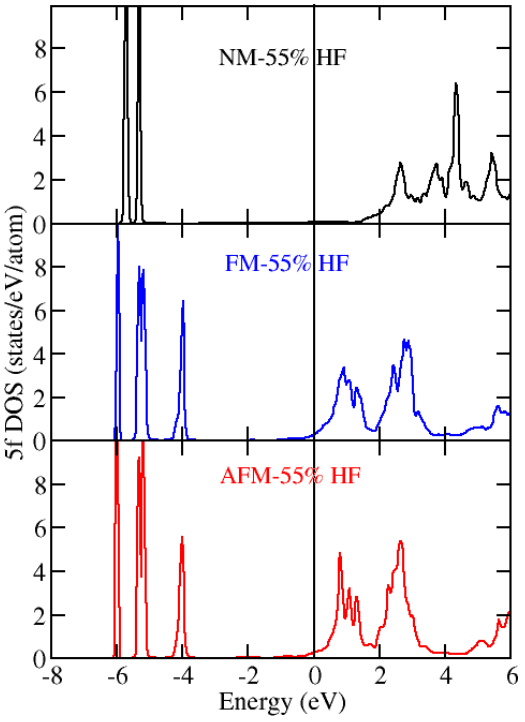


Figure 10a

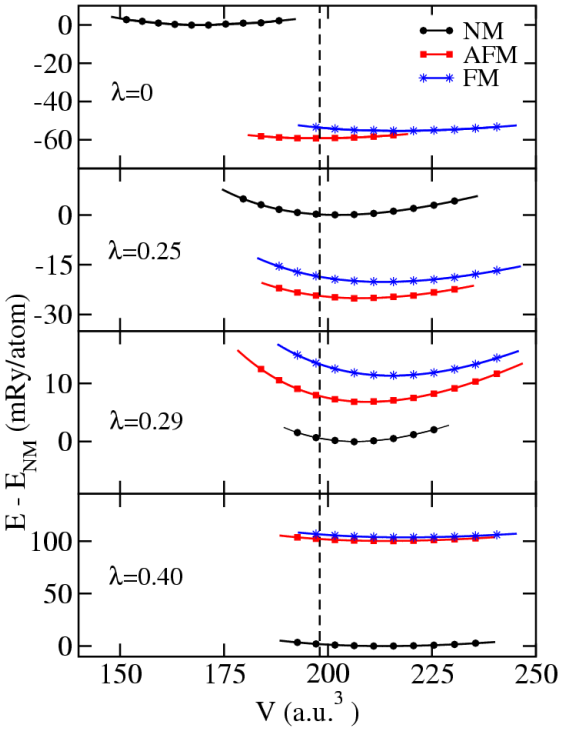

Figure 10b

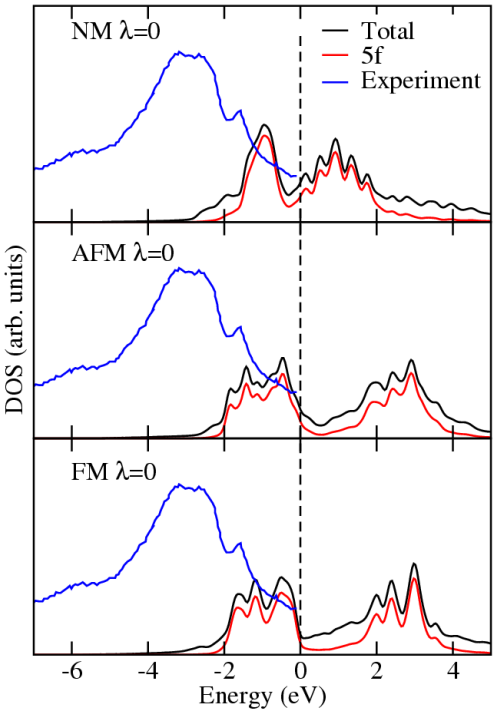


Figure 10c

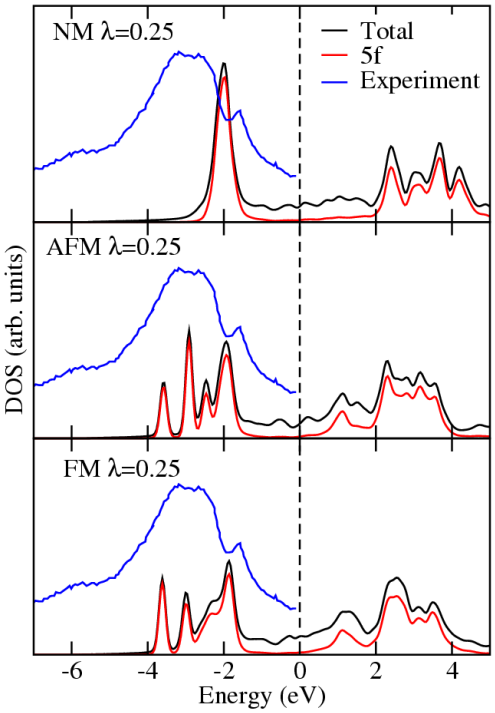


Figure 10d

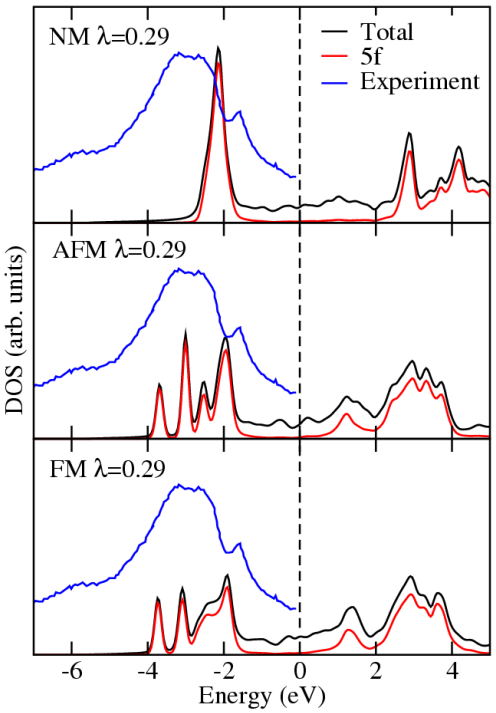


Figure 10e

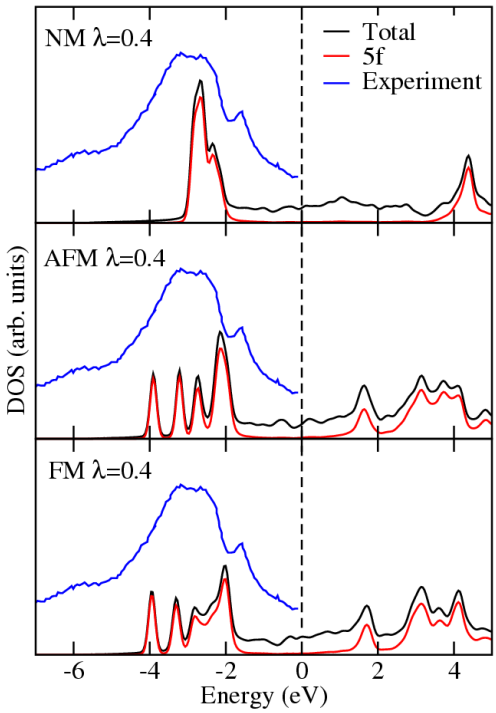

**f) Molecular Hydrogen and Oxygen Adsorption on the (0001) Surface of Doble-Hexagonal-Close-Packed (dhcp) Am**

The dhcp-Am (0001) surface was modeled by a supercell consisting of a periodic 6-layer slab with a (2×2) surface unit cell and vacuum of 30 Bohr thickness. Using bulk optimized lattice constants, a 2x2 hexagonal surface unit cell (2 atoms along each lateral 2D direction yielding 4 Am atoms per surface unit cell) for (0001) orientation was constructed. The surface was then relaxed (Fig. 11), with the reduction in the total energy of the slab being only 2.19 mRy. In Figure 12, the Gaussian-broadened (with a width of 0.045 eV) *f* and *d* LDOS curves for each of the layers of the bare dhcp Am (0001) metal slab are shown. Clearly, we see well-defined peaks in the 5*f* electron LDOS in the vicinity of the Fermi level, which have also been observed for bulk dhcp-Am(0001), and is a clear signature of 5*f* electron localization. Also, the $5f_{5/2}$ electron localization is more pronounced for the surface and subsurface layers than the central layer. As an example of the modified DOS for atomic adsorptions, we show in Figure 13 that for oxygen adsorption, hybridizations lead to modifications in the 5*f* DOS below the Fermi level at the top site.

For molecular adsorption, the admolecule, corresponding to a surface coverage of Θ = 1/4 of a monolayer (ML), was allowed to approach the surface from both sides to preserve inversion symmetry. Three high symmetry adsorption sites were considered: (i) one-fold top site t1 (admolecule is directly on top of an Am atom) (ii) two-fold bridge site b2 (admolecule is placed in the middle of two nearest neighbor Am atoms); and (iii) three-fold hollow hcp site h3 (admolecule sees a Am atom located on the layer directly below the surface layer). For each of these three adsorption sites, three approaches of the $H_2$ molecule towards to the surface were considered: (a) approach vertical to the surface (Vert approach) (Figure 14); (b) approach parallel to a lattice vector (Hor1 approach) (Figure 15); (c) approach perpendicular to a lattice vector (Hor2 approach) (Figure 16). For all configurations studied, the adsorption was found to be molecular, with the highest adsorption energy being 0.1 eV with a H-H distance of 0.79 Å at the fully relativistic level for both the Hor1 and Hor2 approaches at the top site. Also, increasing stability at both the NSOC and SOC levels of theory implied decreasing vertical distance ($R_D$) of the $H_2$ molecule from the surface layer. The primary conclusion is that irrespective of the $H_2$ molecule approach, the most favorable configuration is the one with the smallest $R_D$. This is true for the Vert, Hor1 and Hor2 cases. The smallest value of $R_D$ is 2.65 Å for the most stable case.

To understand the dissociation process of the hydrogen molecule on the (0001) surface of dhcp-Am, we studied the reaction barrier by constraint minimization of the total energy along a chosen reaction coordinate. We have calculated the reaction barrier for only the most favorable adsorption site t1 for the Hor2 approach. Figure 17 shows the optimized energy curve with respect to different H – H distances. The first minima of the curve shows the molecular adsorption of hydrogen near the optimized $H_2$ bond length of 0.789 Á. The second minima occur at an H – H distance of 3.547 Á, where each hydrogen atom sits nearly on two three-fold h3 adsorption sites with an adsorption energy of 0.8298 eV. The curve has maxima at a H – H distance of 1.6 Á, and between the two minima's of the curve, there exists an energy hill of 0.142 eV. This energy is defined as the activation energy to be supplied at 0 K to the $H_2$ molecule for the dissociation process to proceed. After dissociation, the adsorption is primarily atomic in nature. Also, this is consistent with our previous finding for the adsorption of atomic hydrogen where the three-fold hcp site was found to be most favorable and in the current work

the hydrogen molecule dissociates to two three-fold h3 adsorption sites giving the most stable configuration.

For oxygen adsorption, for the Vert approach, the adsorption process is molecular in nature. On the other hand, for both Hor1 and Hor2 approaches, the adsorption is dissociative (Figure 18). The figure is shown as A → B + C, where A is the initial adsorption site (the center of mass of $O_2$ was initially placed at this site) and B and C are the final adsorption sites (each atom of the dissociated molecule sits at this site). The three dissociated configurations corresponding to the three initial adsorption sites t1, b2 and h3 are: (a) t1 → b2 + b2; (b) b2 → t1 + t1; (c) h3 → b1 + b1, respectively. Regarding the chemisorption energies, the most stable configuration is the t1 → b2 + b2 dissociation (8.681 eV for the NSOC case, 9.191 eV for SOC case), followed by the h3 → b1 + b1 dissociation (6.564 eV for the NSOC case, 7.057 eV for SOC case), with the least favorable site being b2 → t1 + t1 (5.472 eV for the NSOC case, 5.861 eV for SOC case). Similar to the trend for the Vert approach, increasing stability at both the NSOC and SOC cases implies decreasing vertical distance of the $O_2$ molecule from the surface layer.

For the Hor2 approach, where the $O_2$ molecular approach is horizontal but perpendicular to a lattice vector, the following dissociative configurations were observed: (a) t1 → h3 + h3; (b) b2 → h3 + f3; (c) h3 → t1 + b2. The most energetically stable configuration corresponds to the t1 → h3 + h3 dissociation (9.395 eV for the NSOC case, 9.886 eV for SOC case), followed by the dissociation b2 → h3 + f3 (8.972 eV for the NSOC case, 9.456 eV for SOC case), with the least energetically favorable configuration being the dissociation h3 → t1 + b2 (5.615 eV for the NSOC case, 6.084 eV for SOC case). For the most favorable configuration for Hor2 approach, t1 → h3 + h3, which is also the most favorable configuration among all the three approaches, we also studied the reaction pathway for the dissociation of oxygen molecule to the most stable hollow sites and no existence of any energy barrier was found.

Differential partial charge analyses tend to suggest that *some* of the Am 5*f* electrons participate in chemical bonding. For the Hor1 approach corresponding to t1→b2+b2 in Figure 19, and similarly for Hor2 approach corresponding to t1→ h3+h3, the Am-O bonds are again largely ionic in character as significant charge accumulation around the O atoms can be

Figure 11

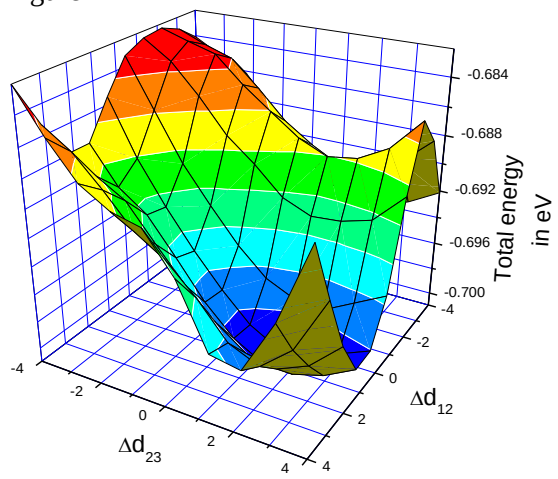


Figure 12

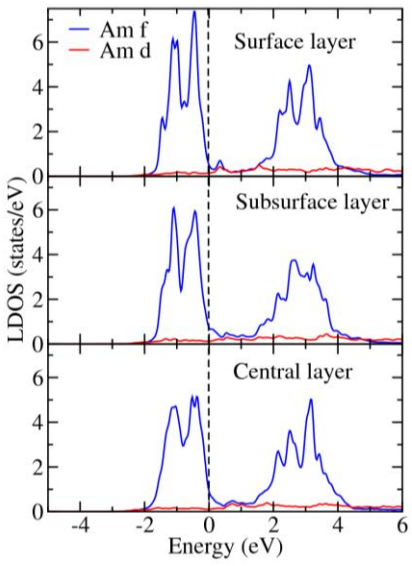

Figure 13

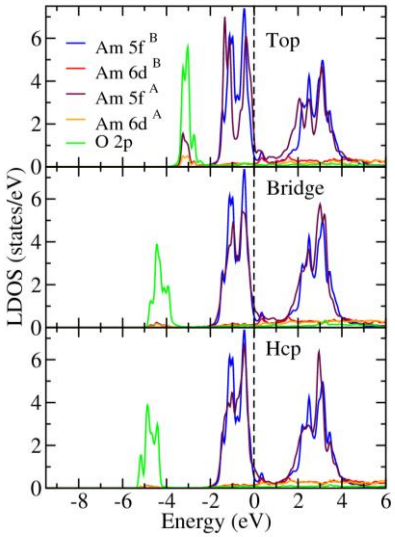


Figure 14

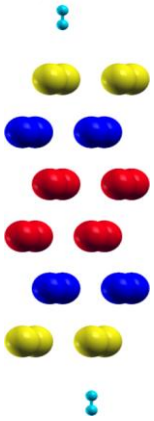

Figure 15

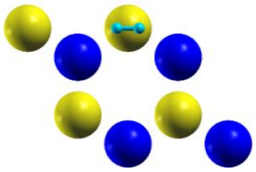

Figure 16

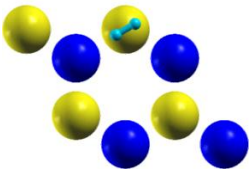

Figure 17

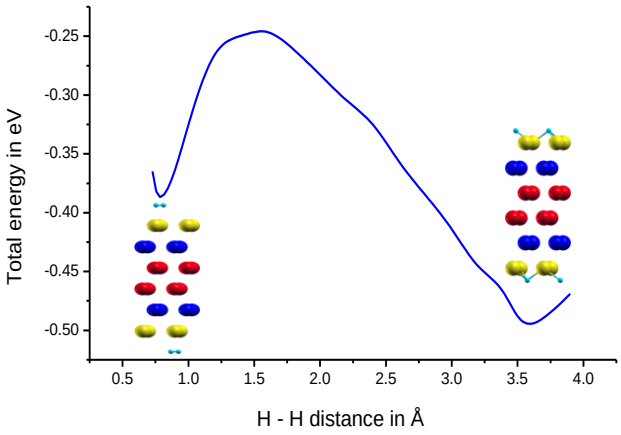


Figure 18

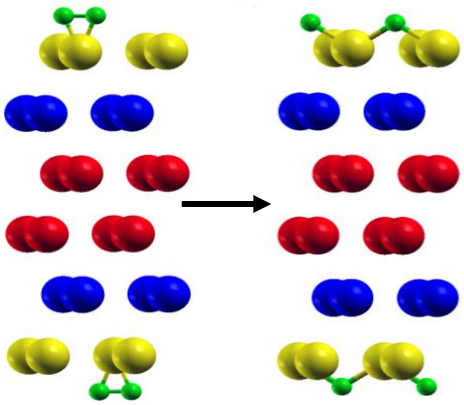

Figure 19

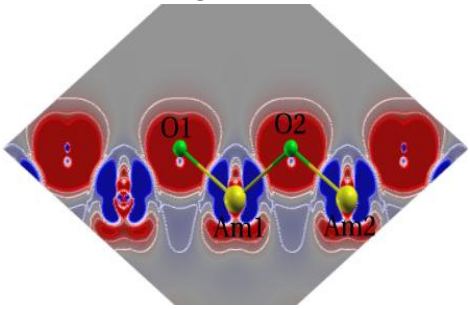


Figure 20

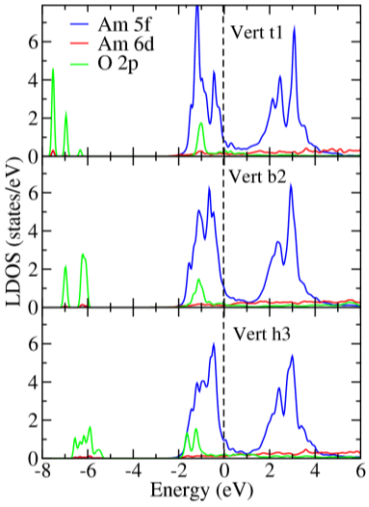

observed. The difference charge density plots are fairly consistent with the positive changes in the work function as well as the differential partial charges. We also computed the local density of states (LDOS). In all cases, we observe a broadening in the 5*f* band peaks below the Fermi level when compared to the bare surface (Figure 20). Furthermore, a fair amount of O(2*p*) and Am(6*d*, 5*f*) hybridizations are evident. We hasten to point out that overall, the Am 5*f* states for all the Vert, Hor1, and Hor2 approaches show signatures of *slight* delocalization.

**g) On the interplay between spin polarization, orbital polarization and spin-orbit coupling in actinides from Pa to Cm**

We have also performed a systematic investigation of the effects of spin polarization, orbital polarization and spin-orbit coupling in six actinide elements, namely protactinium (Pa), uranium (U), neptunium (Np), plutonium (both $\alpha$-Pu and $\delta$-Pu), americium (Am) and curium (Cm) using a relativistic full-potential augmented plane wave with local orbital basis method. For each element, these effects have been investigated for non-magnetic (NM), ferromagnetic (FM) and anti-ferromagnetic (AFM) arrangements. Also, each of these three magnetic orders has been studied at three levels of approximations, specifically without spin-orbit coupling (NSO), with spin-orbit coupling (SO) and with orbital polarization (SO + OP). These effects originate from delicate interplay between kinetic energy of *5f* electrons, spin-orbit coupling, minimization of onsite coulomb interaction, and magnetization resulting from inter-site correlation. Our calculation shows that the *5f* electrons in lighter actinides (Pa, U, Np) are strongly itinerant with no magnetic effects. In heavier actinides (Am, Cm), the *5f* electrons are strongly correlated and quite sensitive to spin polarization, although the difference between FM and AFM energies tends to be very small. The orbital polarization has strongest effect in NM order and nearly vanishes for spin polarized calculations in almost all cases. The *5f* electrons in $\alpha$-Pu are close to being delocalized and their behavior is similar to that of lighter actinides (Fig. 21). Among all the elements studied in this work, $\delta$-Pu exhibits the most complex behavior. All forms of correlation effects are comparable in $\delta$-Pu and significantly affect volume, bulk modulus and ground state energy.

**h) An LDA+*U* study of the photoemission spectra of the ground state phases of Am and Cm**

We have investigated the photoemission spectra and other ground state properties such as equilibrium volume, bulk modulus, and the magnetic and electronic properties α-Am and α-Cm (both of which have double hexagonal close packed crystal structure) using the LDA+*U* method as implemented in *WIEN2k*. The method consists of identifying orbitals with atomic-like characteristics and treating them with an LDA-corrected method by adding an orbital-dependent on-site Coulomb repulsion (via the Hubbard *U*) to the DFT Hamiltonian and subtracting the so-called double counting (dc) correction. The dc correction was treated within the self-interaction-corrected scheme. As is known, DFT predicts a magnetic ground state with sizable moments (experimentally α-Am is paramagnetic) and a qualitatively wrong 5*f* DOS (in comparison to the photoemission spectra) due largely to the incorrect treatment of the localized 5f electrons. Strictly speaking, the LDA+*U* scheme is not fully *ab initio* since U effectively becomes a parameter that must be adjusted to get a property of interest. Nevertheless it is accepted as a realistic alternative to DFT for materials with localized *d* and *f* electrons.

Our LDA+*U* calculations show that spin polarized americium is energetically favorable but spin degenerate configuration produces *some* experimental quantities significantly better than those calculated using the spin polarized configuration. The photoemission spectra (PES)

are primarily used as a benchmark for the success of the calculation of the strongly correlated materials. As indicated in Figure 22, in which the density of states calculated using LDA+*U* are shown alongside dynamical mean-field theory results[255] and experimental PES[236], the non-magnetic DOS is in good agreement with experimental PES when U=4.5 eV. In particular, the elusive 5*f* band center of gravity at around 3 eV below the Fermi level is well reproduced. In spin polarized case, the onsite interaction parameter, *U*, is observed to increase the splitting between occupied and unoccupied bands by enhancing the Stoner parameter (in pure LSDA calculations, the Stoner parameter is responsible for splitting between the occupied and unoccupied bands). The DOS of anti-ferromagnetic curium is shown to be in good agreement with that calculated using dynamical mean-field theory[174] for *U*=3.5 eV (Figure 23). For curium exchange interaction appears to play a dominant role in its magnetic stability.

Figure 21

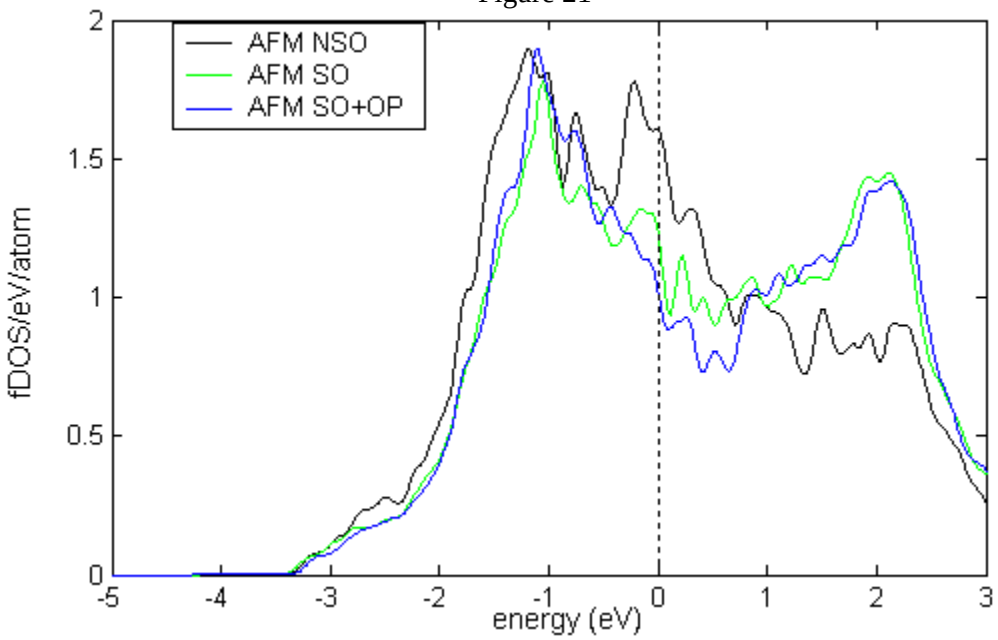


Figure 22

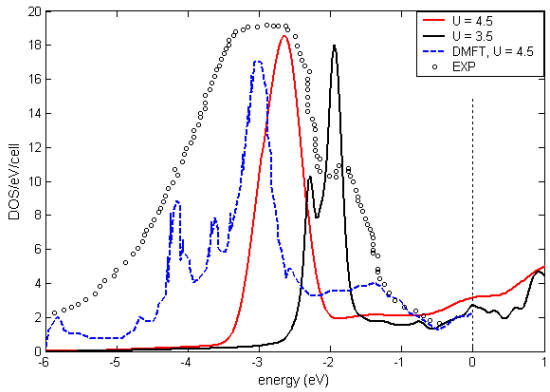


Figure 23

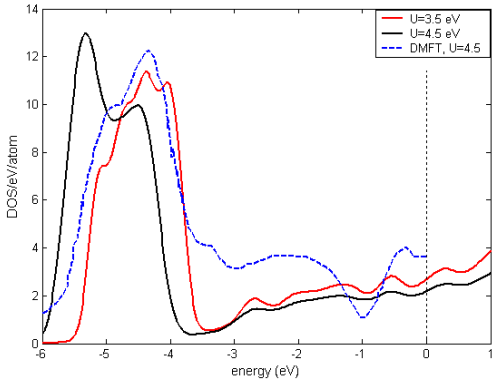

## Publications from 2006 to 2010

[1] H. R. Gong and A. K. Ray, "*A First-Principles Study of the (111), (001), and (110) Surfaces of δ – Pu*," Actinides 2005 – Basic Science, Applications and Technology, MRS Symposium Proceedings, **803**, 44-50 (2006).

[2] D. Gao and A. K. Ray, "*The 5f Localization – Delocalization in Square and Hexagonal Americium Monolayers – A FP-LAPW Electronic Structure Study*," European Physical Journal B, **50**, 497-503 (2006).

[3] H. R. Gong and A. K. Ray, "*A Fully-Relativistic Full-Potential-Linearized-Augmented-Plane-Wave Study of the (111) Surface of δ - Pu,*" Surface Science, **600**, 2231-2241 (2006).

[4] D. Gao and A. K. Ray, "*On the Convergence of the Electronic Structure Properties of the FCC Americium (001) Surface*," Surface Science, **600**, 4941-4952 (2006).

[5] R. Atta-Fynn and A. K. Ray, **"***A Full Potential–Linearized Augmented Plane Wave (FP-LAPW) Study of Atomic Carbon, Nitrogen, and Oxygen Chemisorption on the (100) Surface of δ-Pu*," Physica B, **392**, 112-126(2007).

[6] A. K. Ray and P. Dholabhai, "*A Density Functional Study of Atomic Oxygen and Carbon Adsorptions on (100) Surface of γ – Uranium*," Physica Scripta, **75**, 506-514 (2007).

[8] D. Gao and A. K. Ray, **"***Quantum Size Effects in the (0001) Surface of Double Hexagonal Close Packed Americium,"* European Physical Journal B, **55,** 13-22 (2007).

[9] R. Atta-Fynn and A. K. Ray, "*An Ab Initio Full Potential Fully Relativistic Study of Atomic Carbon, Nitrogen, and Oxygen Chemisorption on the (111 Surface of δ -Pu*," Physical Review B, **75**, 195112-1-13 (2007).

[10] D. Gao and A. K. Ray, "*A First-Principles Electronic Structure Study of the High-Symmetry Surfaces of FCC Americium*," Journal of Alloys and Compounds, **444-445**. 184-190 (2007).

[11] A. K. Ray and P. Dholabhai, "*A Density Functional Study of Carbon Monoxide Adsorption on the (100) Surface of γ-Uranium,*" Journal of Alloys and Compounds, **444-445**. 356-362 (2007).

[12] R. Atta-Fynn and A. K. Ray, "*A Fully Relativistic Density Functional Study of the Actinide Nitrides,*" Physical Review B, **76**, 115101-1-12 (2007).

[13] R. Atta-Fynn and A. K. Ray, **"***Relaxation of the (111) Surface of δ – Pu and Effects on Atomic Adsorption – An Ab Initio Study*," Physica B, **400**, 307-316 (2007).

[14] H. R. Gong and A. K. Ray, "*First Principles Calculations of Localization of 5f Electrons in Bulk Alpha-Plutonium*," Journal of the Physical Society of Japan, **76**, 114701-1-4 (2007).

[15] D. Gao and A. K. Ray, "*A Relativistic Density Functional Study of FCC Americium and the (111) Surface*," Physical Review B, **77**, 035123-1-9 (2008).

[16] R. Atta-Fynn and A. K. Ray, "*Atomic Adsorption on the (020) Surface of α – Pu – A Density Functional Study*," Physical Review B, **77**, 085105-1-11 (2008).

[17] R. Atta-Fynn, P. Dholabhai, and A. K. Ray, "*A Density Functional Study of Atomic Hydrogen and Oxygen Chemisorption on the Relaxed (0001) Surface of Double Hexagonal Close Packed Americium*," European Physical Journal B, **61**, 261-270 (2008).

[18] R. Atta-Fynn, P. Dholabhai, and A. K. Ray, "*An Ab Initio Study of the Adsorption and Dissociation of Molecular Oxygen on the (0001) Surface of Double Hexagonal Close Packed Americium*," Physica B, **403**, 4269-4280 (2008).

[19] R. Atta-Fynn and A. K. Ray, "*Does Hybrid Density Functional Theory Predict a Non-Magnetic Ground State for δ-Pu?*," Europhysics Letters, **85**, 27008-1-6 (2009).

[20] P. Dholabhai and A. K. Ray, **"***Adsorption and Dissociation of Molecular Hydrogen on the (0001) Surface of Double Hexagonal Close Packed Americium*," European Physical Journal B, **67**, 183-192 (2009).

[21] P. Dholabhai and A. K. Ray, **"***Adsorption and Dissociation of Water on the (0001) Surface of Double Hexagonal Close Packed Americium*," Physica Status Solidi B, **246**, 1225-1237 (2009).

[22] F. Islam and A. K. Ray, "*Interplay between Spin Polarization, Orbital Polarization, and Spin-Orbit Coupling in Actinides from Pa to Cm*," Journal of Computational and Theoretical Nanoscience, **6**, 1458-1467 (2009).

[23] R. Atta-Fynn and A. K. Ray, "*A Relativistic DFT Study of Water Adsorption on δ-Pu (111) Surface*," Chemical Physics Letters, **470**, 233-239 (2009).

[24] R. Atta-Fynn and A. K. Ray, "*A First Principles Study of the Adsorption and Dissociation of $CO_2$ on the δ-Pu (111) Surface*," European Physical Journal B, **70**, 171-184 (2009).

[25] R. Atta-Fynn and A. K. Ray, "*Probing the 5f Electrons in Am-I by Hybrid Density Functional Theory,"* Chemical Physics Letters, **482**, 223-227 ((2009).

[26] F. Islam and A. K. Ray, "*An LDA+U Study of the Photoemission Spectra of the Double Hexagonal Close Packed Phases of Am and Cm,"* Solid State Communications, **150**, 936-942 (2010).

[27] J. Wang, Li Ma, and A. K. Ray, "*On the Magnetic and Thermodynamic Properties of Americium II – A Hybrid Density Functional Theoretic Study,"* Physics Letters A, **374**, 4704-4712 (2010).

[28] R. Atta-Fynn and A. K. Ray, "*A Hybrid DFT Description of the (0001) Surface of Americium I,"* European Physical Journal B , **78**, 13-22 (2010).

[29] F. Islam and A. K. Ray, "*Atomic Hydrogen Adsorption on the (020) Surface of α-Pu – A Computational Study*," Physica Status Solidi B, **248**, 193-202 (2011)

[30] Li Ma and A. K. Ray, "*A Hybrid Density Functional Theory Study of $PuO_{2\pm0.25}$, $UO_{2\pm0.25,}$ $U_{0.5}Pu_{0.5}O_{2\pm0.25,}$* " European Physical Journal B, **81**, 103-113 (2011).

[31] J. Wang and A. K. Ray, "*Adsorption and Dissociation of Molecular Oxygen on α-Pu (020) Surface, "* Physica B, **405**, 3285-3294 (2011).

[32] J. Wang and A. K. Ray, "*A First-Principles Study of Water Adsorption on α-Pu (020) Surface,"* Journal of Nuclear Materials, **424**, 138-145 (2012).

[33] Li Ma and A. K. Ray," *Formation Energies and Swelling of Uranium Dioxide by Point Defects,"* Physics Letters, **376**, 1499-1505 (2012).